SUPPLEMENTARY INFORMATION: Specificity and mechanism-of-action of the JAK2 tyrosine kinase inhibitors ruxolitinib and SAR302503 (TG101348)

1. Determination of binding mode of Ruxolitinib to JAK2 by explicit solvent molecular dynamics (MD)

Methods

The thienopyridine inhibitor in the Jak2 crystal structure (PDB ID 3TJD) was replaced manually by Ruxolitinib. Ruxolitinib and the protein were parameterized by the CHARMM general force field and CHARMM22 protein force field, respectively. The solvent was treated explicitly by TIP3P water molecules. A total of 52 sodium and 53 chloride ions were added to neutralize the system and obtain a salt concentration of 150 mM. Ten independent MD simulations were started with different initial distributions of the velocities. The temperature was kept constant at 310K with the thermostat v-rescale, and the pressure at 1 atm (Berendsen coupling). Particle Mesh Ewald was used for the long range electrostatics and the van der Waals energy was truncated at 10. LINCS was applied on all bond and angles to use the integration time 2fs. An aggregated sampling of 1.5 μs was collected (10 runs of 0.15 μs each). Snapshots were saved every 2 ps for a total of 750,000 coordinate sets. All simulations were carried out with GROMACS. The WORDOM implementation of the sequential leader-like algorithm was used for clustering with a threshold of 0.4 Å on the pairwise coordinate root mean square deviation of all the heavy atoms of Ruxolitinib.

Binding mode

The binding mode of Ruxolitinib is very stable. In particular, the pyrrolo[2,3-d]pyrimidin is always involved in two hydrogen bonds with the hinge region of JAK2 (Figure S1).

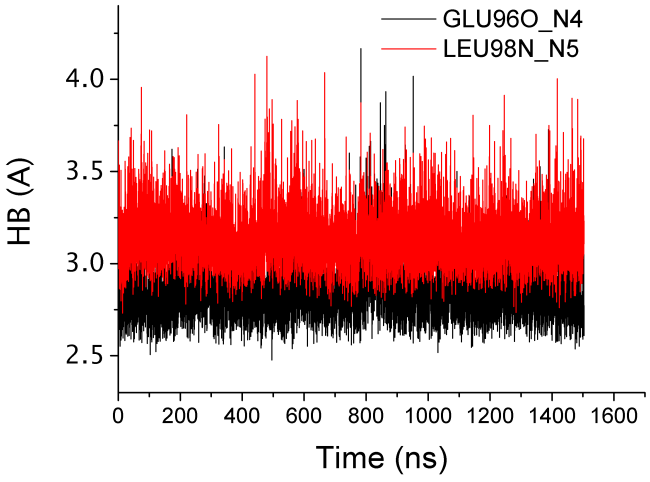

Figure S1. The time series of the hydrogen bonds (HB) between Ruxolitnib and the hinge of JAK2 indicate that both hydrogen bonds are stable.

Free energy profile

The free energy profile shows that there is a major pose and several subbasins (Figure 2). The three rotatable bonds of Ruxolitinib contribute most of the variation on the free energy profile (Figure S3a). The most populated configuration of Ruxolitinib has a weight of about 50% and its unprotonated pyrazole nitrogen is solvent exposed. The cyclopentane forms hydrophobic interaction with the side chain of Val863 and desolvates (i.e., reinforces) the salt bridge between the Asp of the DFG-motif and Lys882 (Figure S4).

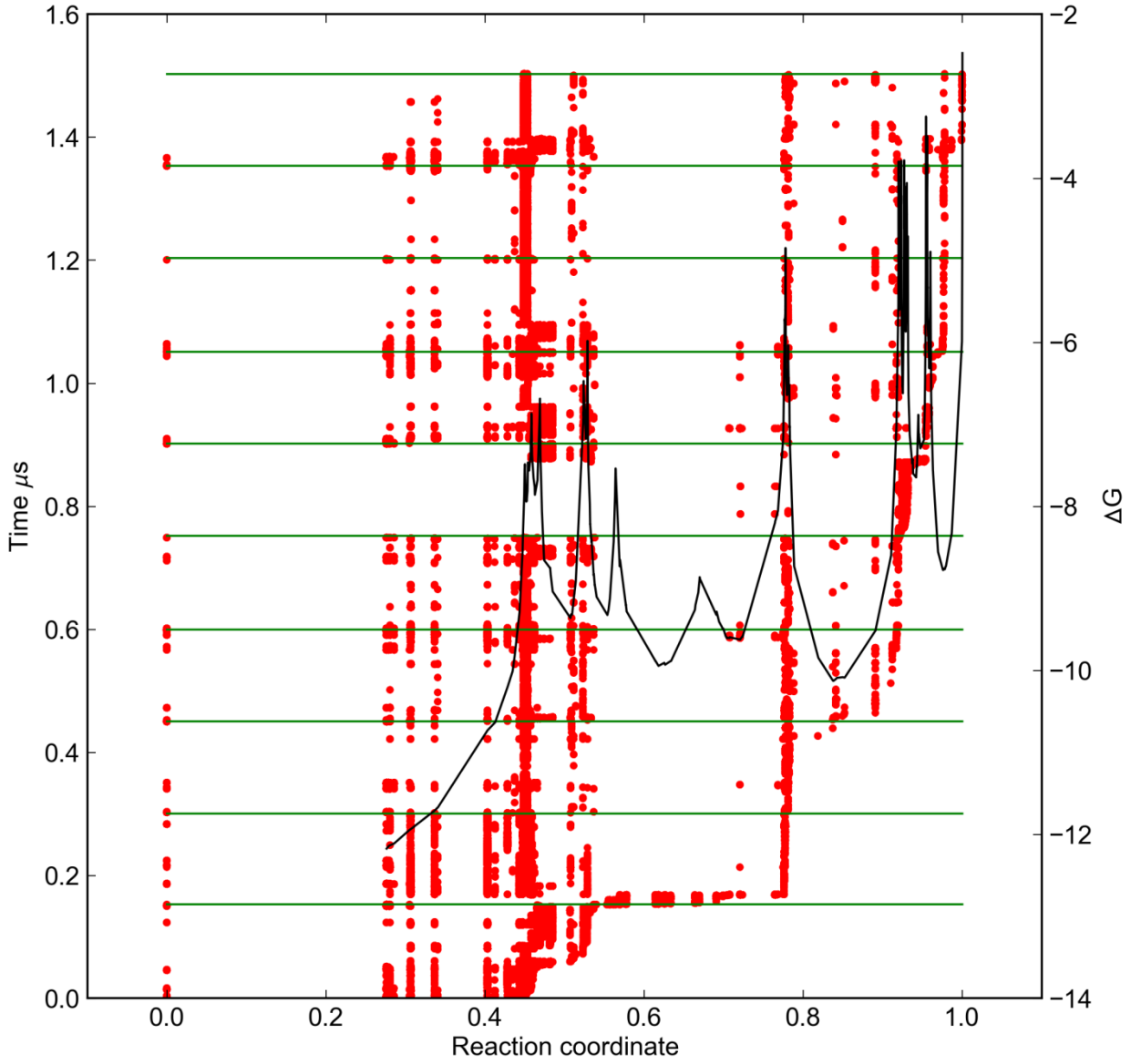

Figure S2 Cut-based free energy profile (black, y-axis on the right) using the most populated cluster as reference. The most populated basin is on the left and includes almost 50% of the molecular dynamics snapshots. The red dots show the time evolution of the binding mode (y-axis on the left) in the individual simulations which are emphasized by green horizontal lines. Multiple transitions between binding modes emerge from the higher frequency of red dots on the barriers separating the individual binding modes.

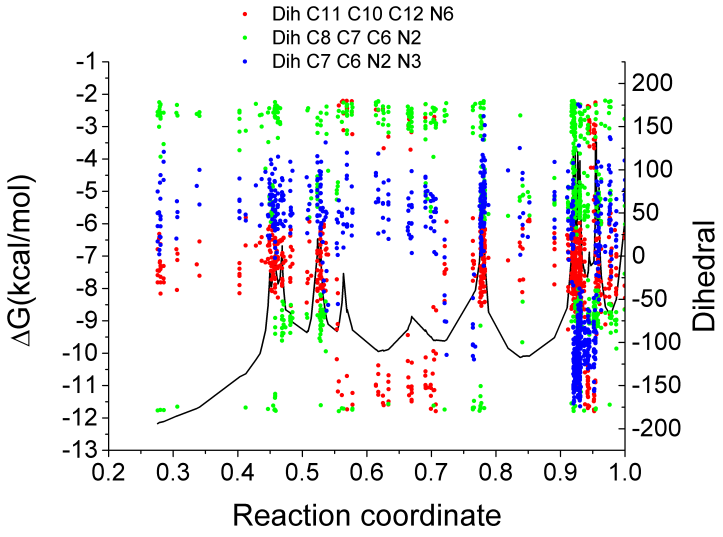

(a)

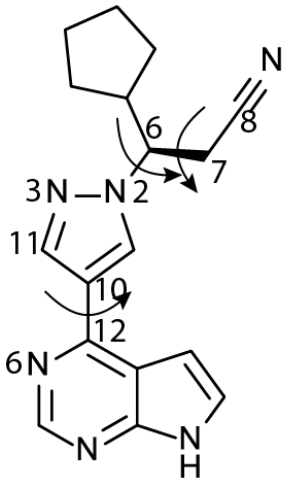

(b)

Figure S3. Cut-based free energy profile and Ruxolitinib conformation in individual poses. (a) The colored dots show the value of the dihedral angle of the three rotatable bonds of Ruxolitinib (y-axis on the right) for each cluster along the cut-based free energy profile (y-axis on the left). As an example, the two sub-basins located in the region of the free energy profile at 0.55 < RC < 0.7 have the pyrazol rotated by about 180 degrees (red dots) with respect to the main pose which corresponds to the first basin on the left of the profile and is populated at about 50%. (b) Chemical structure of Ruxolitinib with its rotatable bonds shown by curved arrows. The atoms that define the dihedral angles are numbered and correspond to those in the legend of panel (a).

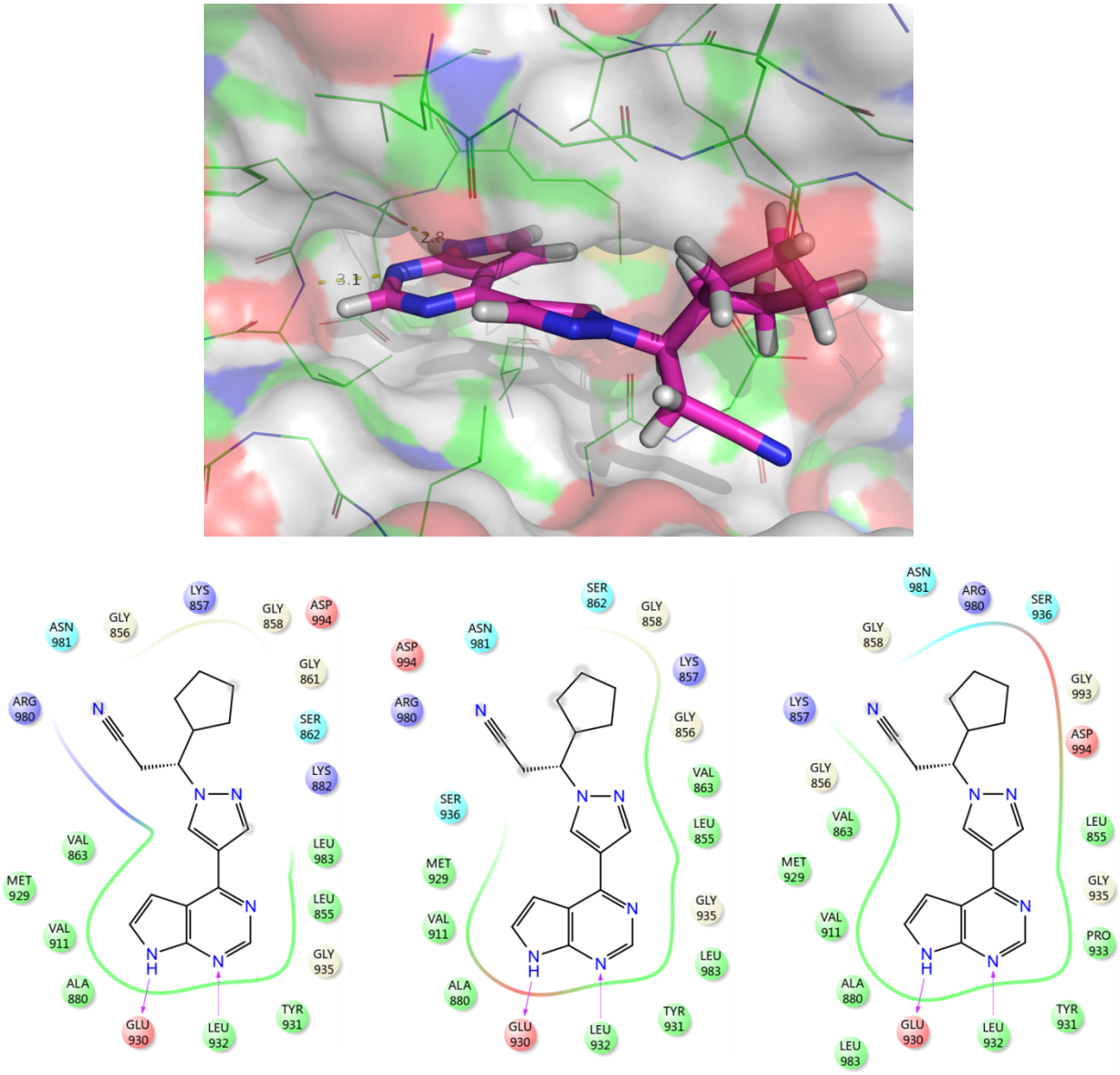

Figure S4. Binding mode of Ruxolitinib into JAK2 as predicted by MD simulations. (Top) Most populated binding mode of Ruxolitinib in the ATP-binding site of JAK2. The hydrogen bonds with the hinge region are shown by dashed lines. The carbon atoms of JAK2 are in green while the carbon, nitrogen, and hydrogen atoms of Ruxolitinib are in magenta, blue, and white, respectively. (Bottom) 2D plots of the three most populated binding modes (from left to right).

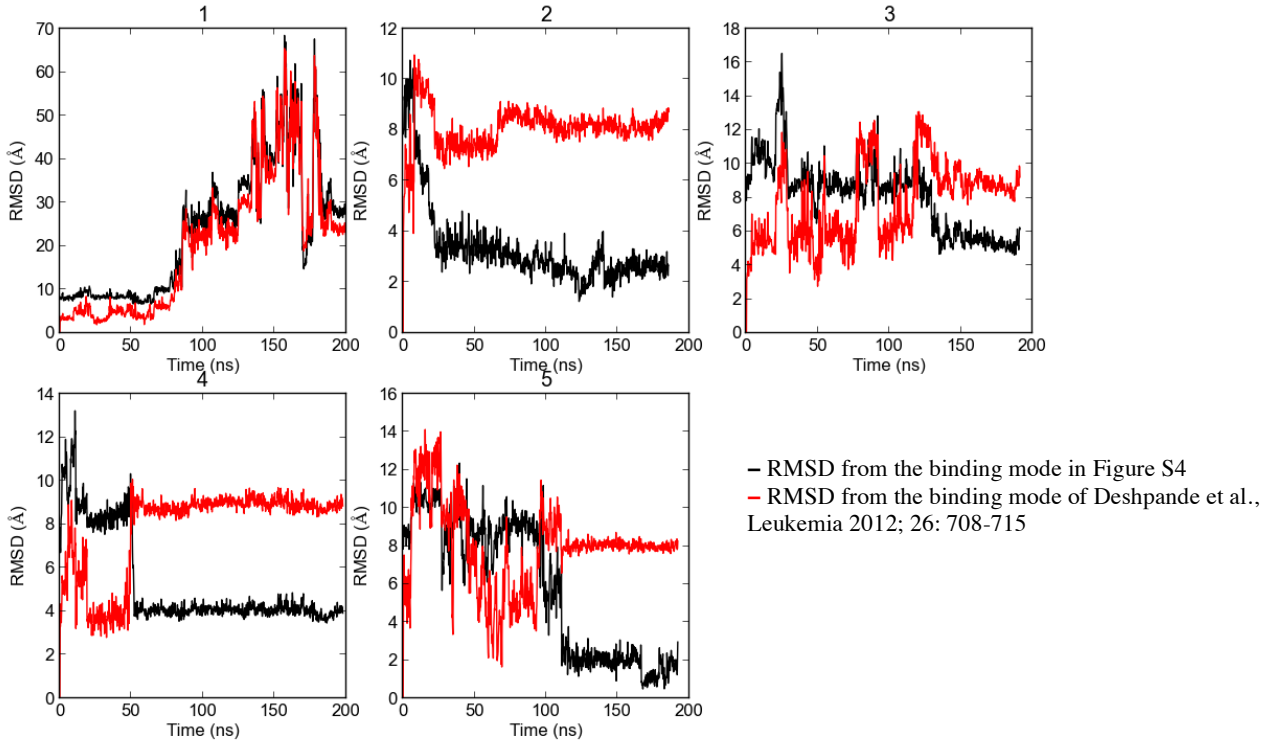

Figure S5. Root mean square deviation (RMSD) of the double-ring system of ruxolitinib from the binding mode proposed in this work (black curve) and the binding mode of Deshpande *et al.*, Leukemia 2012; 26: 708-715 (red curve). Each panel shows a 200-ns MD simulation started from the binding mode of Deshpande *et al*. The five simulations differ in the initial random assignment of the velocities. In all runs, Ruxolitinib dissociates from JAK2 within the first 70 ns which provides strong evidence that the binding mode of Deshpande *et al*. is not stable. Notably, in two of the five simulations (runs 2 and 5), ruxolitinib rebinds with its double-ring system involved in two persistent hydrogen bonds with the hinge region of JAK2 as in Figure S4.

2. Determination of binding mode of SAR302503 to JAK2 by explicit solvent molecular dynamics (MD)

Methods

The thienopyridine inhibitor in the Jak2 crystal structure (PDB ID 3TJD) was replaced manually by SAR302503. SAR302503 and the protein were parameterized by the CHARMM general force field and CHARMM22 protein force field, respectively. The solvent was treated explicitly by TIP3P water molecules. A total of 52 sodium and 54 chloride ions were added to neutralize the system and obtain a salt concentration of 150 mM. Twenty independent MD simulations were started with different initial distributions of the velocities, in ten of which SAR302503 were docked into the conformation that pyrrolidin points to the solvent ("P" conformation, left of Figure S7). In the other ten simulations, the SAR302503 was flipped by about 180 degrees, i.e., the benzenesulfonamide points to the solvent ("B" conformation, right of Figure S7). The temperature was kept constant at 310K with the thermostat v-rescale, and the pressure at 1 atm (Berendsen coupling). Particle Mesh Ewald was used for the long range electrostatics and the van der Waals energy was truncated at 10 Å. LINCS was applied on all bond and angles to use the integration time step of 2fs. All simulations were carried out with GROMACS. An aggregated sampling of 9.62 μs was collected (the length of simulations ranging from 136ns to 617ns since some simulations were stopped when the compound dissociates). Snapshots were saved every 2 ps for a total of 4,810,000 coordinate sets.

Results

The MD simulations suggest that the "P" pose is more stable than the "B" conformation. SAR302503 unbinds within 0.5 microseconds in only two of the ten independent simulations started from the "P" conformation, whereas it unbinds in seven of the ten simulations started from the "B" conformation (Table S1). Interestingly, in three of the runs started from "B" conformation the inhibitor rebinds to JAK2 in a "P" or "P"-like whereas the opposite is never observed (Table S1 and Figure S6), which indicates that the "P" pose is more favorable than the "B" pose.

Table S1. Summary of simulations of SAR302503. The meaning of abbreviations of conformations: "P" represents the bound conformation that the pyrrolidin points to the solvent; "B" represents the bound conformation that the benzenesulfonamide points to the solvent. In "P" and "B" conformations, the hydrogen bonds are formed between N^2-phenylpyrimidine-2,5-diamine of SAR302503 and the hinge. "P-" and "B-" represent the conformation that SAR302503 stays in the binding pocket in "P" and "B"-like conformation, respectively, but the hydrogen bonds which connect SAR302503 and the hinge are lost. "U" represents the unbound conformation.

Simulation	Starting Conf.	End Conf.	Length (ns)
1	P	U	175
2	P	P-	604
3	P	P-	469
4	P	P-	594
5	P	P	617
6	P	P	462
7	P	P-	465
8	P	P	494
9	P	U	460
10	P	P	581
11	B	U	514
12	B	B-	544
13	B	P-	534
14	B	P-	525
15	B	B	522
16	B	B-	518
17	B	P	511
18	B	U	514
19	B	U	385
20	B	U	136

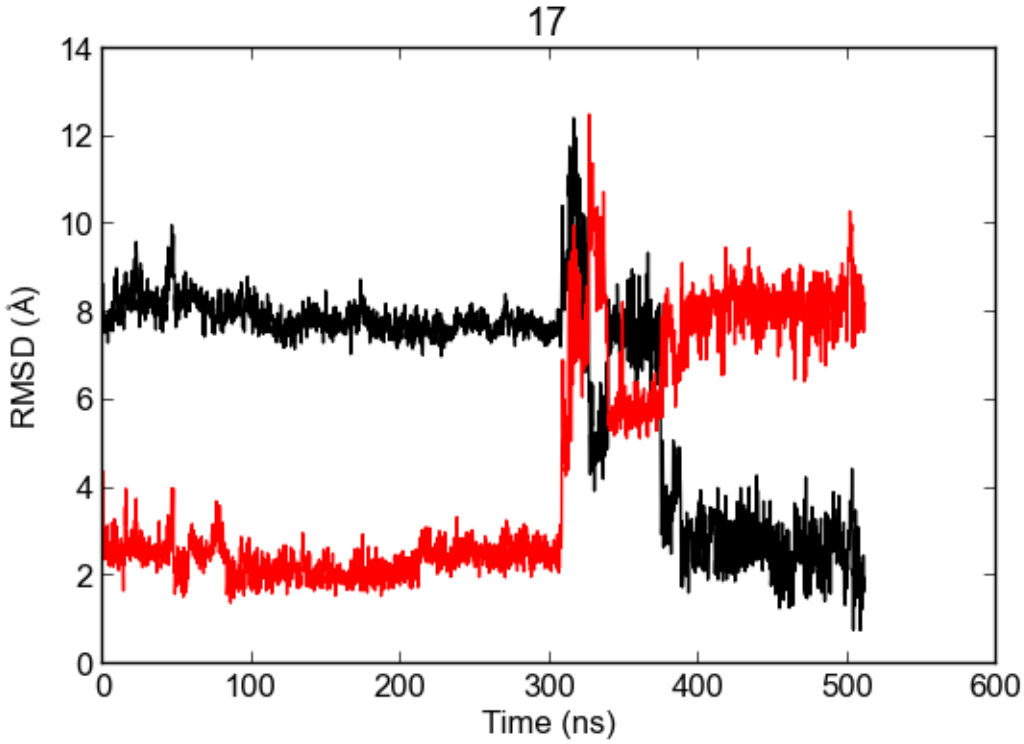

Figure S6. Root mean square deviations (RMSD) of the unsymmetrical heavy atoms of SAR302503 with respect to "P" conformation (black) and "B" conformation (red) in run 17 (Table S1), where a complete conversion of SAR302503 from the "B" conformation to the "P" conformation was observed. The complex of SAR302503 and JAK2 was fitted based on all carbon alphas of the protein before calculating the RMSD. The reference structure for the red time series is the "B" conformation reached at the end of run 15, while the black curve is the time series of RMSD with respect to the "P" conformation reached at the end of run 17.

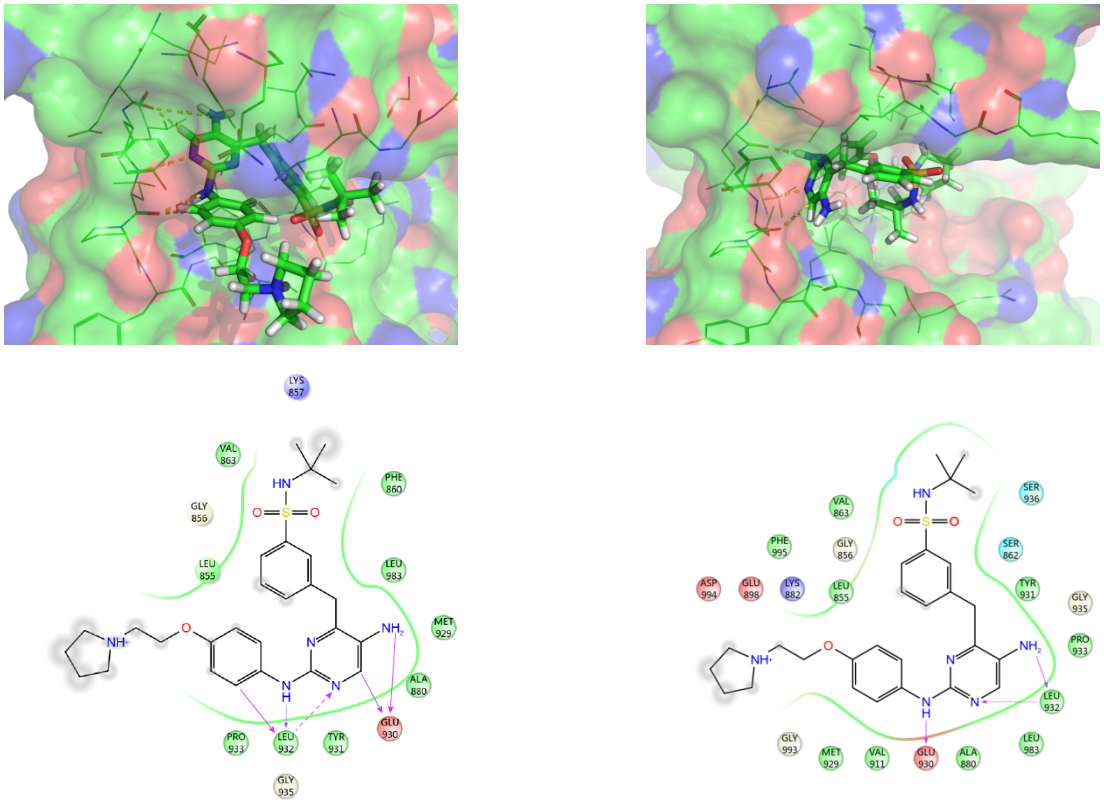

"P" conformation "B" conformation

Figure S7. Two possible binding modes of SAR302503. The SAR302503 is depicted in stick models, whereas JAK2 is depicted in surface model. The color of the surface model depends on the atomic element contributing to the surface, i.e., carbons are in green, oxygens are in red, and nitrogens are in blue. Hydrogens of the protein are omitted for clarity.

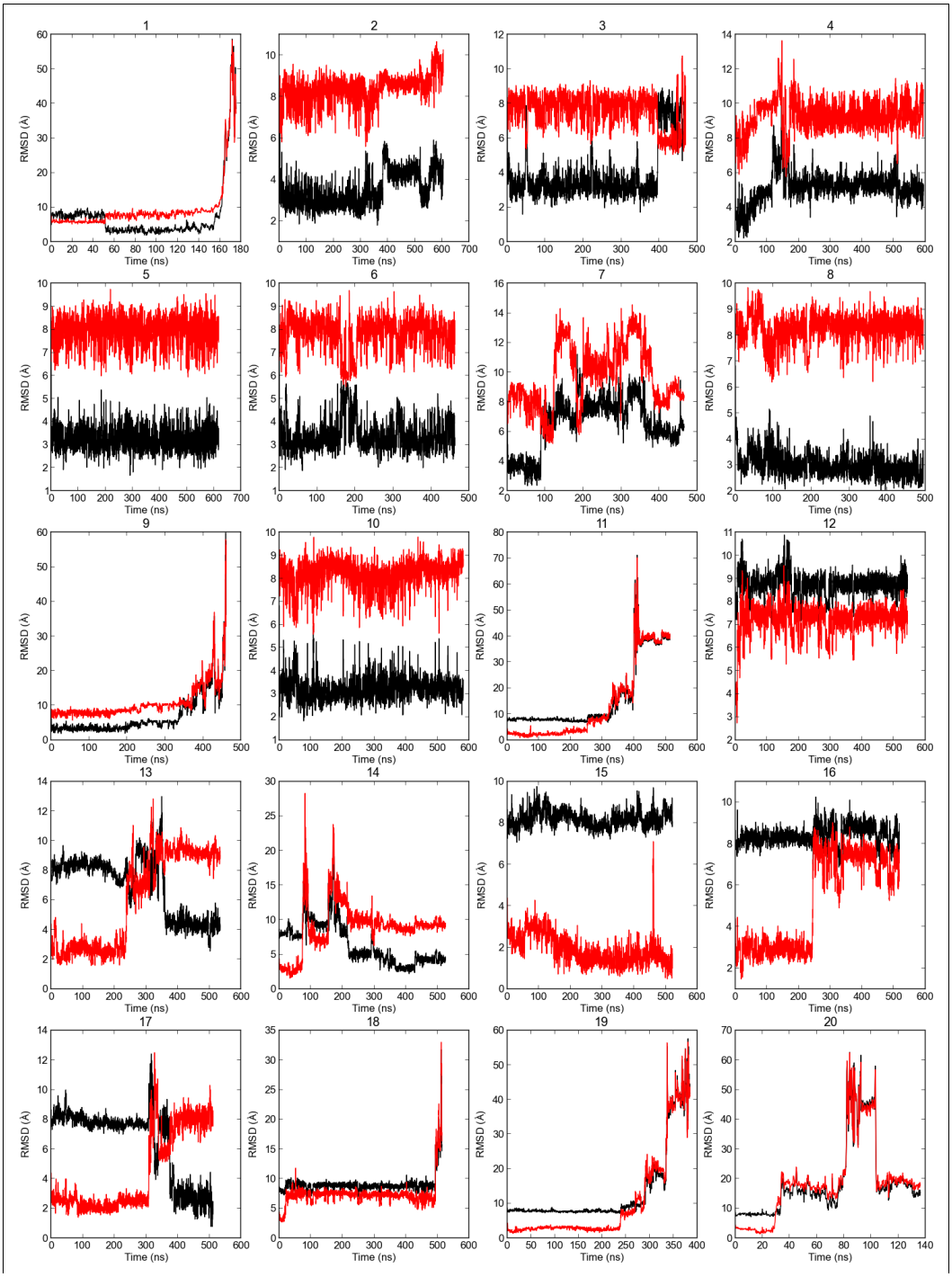

Figure S8. RMSD of the unsymmetrical heavy atoms of SAR302503 with respect to "P" conformation （black curve） and "B" conformation (red curve) in all 20 simulations. The complex of SAR302503 and JAK2 was fitted based on all carbon alphas of the protein before calculating the RMSD. The red curve is the time series of RMSD with respect to the "B" conformation where the 15th simulation finished; the black curve is the time series of RMSD with respect to the "P" conformation where the 17th simulation finished. These simulations indicate that the P binding mode is more stable than the B binding mode.

Table S1a: Profiling SAR302503 (TG101348) and Ruxolitinib at 1μM concentration against 358 protein kinases, d

Residual activities (% of control)
Mean residual activity < 50 %

#	Kinase Name	Kinase Family*	Cpd ID	SAR302503, repeat 1	SAR302503, repeat 2	Mean	Ruxolitinib, repeat 1	Ruxolitinib, repeat 2	Mean
			Assay Conc. (M)	1.0E-06	1.0E-06	1.0E-06	1.0E-06	1.0E-06	1.0E-06
1	ABL1 E255K	TK		73	75	74	102	105	104
2	ABL1 F317I	TK		98	97	97	106	104	105
3	ABL1 G250E	TK		79	87	83	99	102	101
4	ABL1 H396P	TK		82	86	84	103	98	100
5	ABL1 M351T	TK		68	71	69	92	92	92
6	ABL1 Q252H	TK		84	84	84	98	105	101
7	ABL1 T315I	TK		83	85	84	101	99	100
8	ABL1 wt	TK		65	67	66	100	95	97
9	ABL1 Y253F	TK		68	72	70	108	104	106
10	ABL2	TK		67	70	68	82	93	87
11	ACK1	TK		13	13	13	28	28	28
12	ACV-R1	TKL		10	10	10	85	84	85
13	ACV-R1B	TKL		88	85	87	99	86	92
14	ACV-RL1	TKL		14	15	14	91	73	82
15	AKT1	AGC		105	96	101	110	96	103
16	AKT2	AGC		107	98	103	86	88	87
17	AKT3	AGC		111	105	108	109	97	103
18	ALK (GST-HIS-tag)	TK		97	94	96	35	27	31
19	AMPK-alpha1	CAMK		73	66	70	81	83	82
20	ARK5	CAMK		55	45	50	101	105	103
21	ASK1	STE		100	104	102	112	90	101
22	Aurora-A	OTHER		69	62	65	83	80	82
23	Aurora-B	OTHER		49	46	47	58	60	59
24	Aurora-C	OTHER		53	56	55	65	71	68
25	AXL	TK		46	47	46	104	101	102
26	BLK	TK		70	68	69	93	85	89
27	BMPR1A	TKL		111	88	99	100	82	91
28	BMX	TK		86	79	82	105	100	103
29	B-RAF V600E	TKL		93	99	96	86	88	87
30	B-RAF wt	TKL		98	105	101	77	97	87
31	BRK	TK		92	98	95	108	94	101
32	BRSK1	CAMK		86	93	90	93	92	93
33	BTK	TK		66	67	67	90	85	87
34	CAMK1D	CAMK		73	77	75	56	60	58
35	CAMK2A	CAMK		68	60	64	14	14	14
36	CAMK2B	CAMK		85	84	84	76	57	67
37	CAMK2D	CAMK		59	52	56	21	18	20
38	CAMK4	CAMK		96	97	97	104	93	98
39	CAMKK1	OTHER		96	87	92	93	97	95
40	CAMKK2	OTHER		86	87	87	123	105	114
41	CDC42BPA	AGC		104	85	95	68	50	59
42	CDC42BPB	AGC		96	90	93	83	80	82
43	CDK1/CycA	CMGC		107	101	104	104	92	98
44	CDK1/CycB1	CMGC		101	97	99	89	112	101
45	CDK1/CycE	CMGC		104	87	96	91	79	85
46	CDK2/CycA	CMGC		98	87	92	98	84	91
47	CDK2/CycE	CMGC		98	84	91	98	85	92
48	CDK3/CycE	CMGC		116	92	104	85	96	90
49	CDK4/CycD1	CMGC		85	89	87	91	101	96
50	CDK4/CycD3	CMGC		86	81	84	100	97	98
51	CDK5/p25NCK	CMGC		109	94	101	101	89	95
52	CDK5/p35NCK	CMGC		96	89	93	101	90	95
53	CDK6/CycD1	CMGC		74	75	75	79	67	73
54	CDK7/CycH/MAT1	CMGC		67	76	72	99	106	102
55	CDK8/CycC	CMGC		98	80	89	75	64	69
56	CDK9/CycK	CMGC		109	98	103	117	96	106
57	CDK9/CycT	CMGC		97	100	99	111	83	97
58	CHK1	CAMK		105	95	100	99	110	104
59	CHK2	CAMK		77	73	75	97	93	95
60	CK1-alpha1	CK1		102	106	104	98	95	97
61	CK1-delta	CK1		95	105	100	89	85	87
62	CK1-epsilon	CK1		99	90	95	90	64	77
63	CK1-gamma1	CK1		91	97	94	89	84	86
64	CK1-gamma2	CK1		107	101	104	101	92	97
65	CK1-gamma3	CK1		112	125	118	98	97	98
66	CK2-alpha1	OTHER		103	96	100	117	93	105
67	CK2-alpha2	OTHER		94	81	87	97	84	91
68	CLK1	CMGC		87	89	88	77	80	78
69	CLK2	CMGC		103	98	100	92	80	86
70	CLK3	CMGC		87	81	84	76	68	72
71	CLK4	CMGC		92	86	89	59	56	57
72	COT	STE		111	102	107	101	121	111
73	CSF1-R	TK		73	61	67	45	45	45
74	CSK	TK		126	119	122	105	100	103
75	DAPK1	CAMK		17	15	16	50	37	43
76	DAPK2	CAMK		22	21	21	48	50	49
77	DAPK3	CAMK		4	3	4	35	33	34
78	DCAMKL2	CAMK		103	83	93	56	49	53
79	DDR2	TK		35	43	39	73	72	73
80	DMPK	AGC		109	104	107	91	82	86
81	DNA-PK	ATYP		103	94	98	101	98	99
82	DYRK1A	CMGC		109	99	104	105	100	102
83	DYRK1B	CMGC		102	78	90	90	88	89
84	DYRK2	CMGC		104	91	97	101	103	102
85	DYRK3	CMGC		106	101	103	112	87	100
86	DYRK4	CMGC		97	98	97	106	92	99
87	EEF2K	ATYPICAL		106	101	104	110	102	106
88	EGF-R d746-750	TK		121	119	120	117	95	106
89	EGF-R d747-749/A750P	TK		99	112	105	112	87	99
90	EGF-R d747-752/P753S	TK		115	107	111	104	96	100
91	EGF-R d752-759	TK		129	107	118	109	110	109
92	EGF-R G719C	TK		122	108	115	111	111	111
93	EGF-R G719S	TK		108	104	106	115	100	108
94	EGF-R L858R	TK		87	91	89	138	138	138
95	EGF-R L861Q	TK		119	113	116	115	101	108
96	EGF-R T790M	TK		118	117	118	120	106	113
97	EGF-R T790M/L858R	TK		89	69	79	127	122	124
98	EGF-R wt	TK		111	105	108	118	102	110
99	EIF2AK2	OTHER		80	78	79	96	81	89
100	EIF2AK3	OTHER		87	101	94	108	106	107

101	EPHA1	TK	75	76	75	90	69	80	
102	EPHA2	TK	118	97	107	103	87	95	
103	EPHA3	TK	102	94	98	110	94	102	
104	EPHA4	TK	71	73	72	69	63	66	
105	EPHA5	TK	121	120	121	111	109	110	
106	EPHA7	TK	106	97	101	97	93	95	
107	EPHA8	TK	111	99	105	95	95	95	
108	EPHB1	TK	95	84	90	83	67	75	
109	EPHB2	TK	92	87	90	101	89	95	
110	EPHB3	TK	154	138	146	81	98	90	
111	EPHB4	TK	124	127	125	99	97	98	
112	ERBB2	TK	115	113	114	108	98	103	
113	ERBB4	TK	88	89	88	102	98	100	
114	ERK1	CMGC	104	103	103	89	86	87	
115	ERK2	CMGC	95	97	96	83	77	80	
116	FAK	TK	15	12	14	78	75	76	
117	FER	TK	128	121	124	91	83	87	
118	FES	TK	88	86	87	101	99	100	
119	FGF-R1 V561M	TK	6	6	6	48	56	52	
120	FGF-R1 wt	TK	38	38	38	94	82	88	
121	FGF-R2	TK	44	43	43	81	64	73	
122	FGF-R3 G697C	TK	76	73	74	110	97	104	
123	FGF-R3 K650E	TK	90	85	87	99	96	97	
124	FGF-R3 K650M	TK	99	87	93	100	96	98	
125	FGF-R3 wt	TK	81	82	82	127	121	124	
126	FGF-R4	TK	104	109	106	92	93	93	
127	FGR	TK	51	46	48	108	98	103	
128	FLT3 D835Y	TK	21	23	22	87	94	91	
129	FLT3 ITD	TK	17	17	17	88	90	89	
130	FLT3 wt	TK	75	76	76	122	115	118	
131	FRK	TK	47	58	52	94	82	88	
132	FYN	TK	72	71	72	84	87	85	
133	GRK2	AGC	100	98	99	86	84	85	
134	GRK3	AGC	96	88	92	91	84	87	
135	GRK4	AGC	122	102	112	101	74	87	
136	GRK5	AGC	95	85	90	90	75	83	
137	GRK6	AGC	93	82	88	82	68	75	
138	GRK7	AGC	96	82	89	78	67	72	
139	GSG2	OTHER	109	102	105	91	82	86	
140	GSK3-alpha	CMGC	101	96	98	88	78	83	
141	GSK3-beta	CMGC	116	90	103	104	90	97	
142	HCK	TK	86	85	85	98	97	98	
143	HIPK1	CMGC	106	96	101	108	104	106	
144	HIPK2	CMGC	93	79	86	95	82	88	
145	HIPK3	CMGC	108	90	99	111	105	108	
146	HIPK4	CMGC	57	58	57	93	94	94	
147	HRI	OTHER	56	49	53	107	101	104	
148	IGF1-R	TK	88	92	90	101	94	98	
149	IKK-alpha	OTHER	117	97	107	114	95	104	
150	IKK-beta	OTHER	71	54	62	83	86	85	
151	IKK-epsilon	OTHER	63	52	57	72	68	70	
152	INS-R	TK	98	87	92	97	103	100	
153	INSR-R	TK	87	93	90	101	109	105	
154	IRAK1	TKL	100	79	89	87	77	82	
155	IRAK4 (untagged)	TKL	98	96	97	120	117	119	
156	ITK	TK	43	39	41	91	88	90	
157	JAK1	TK	29	27	28	4	2	3	
158	JAK2	TK	2	2	2	0	1	1	
159	JAK3	TK	42	41	41	4	3	4	
160	JNK1	CMGC	40	44	42	103	104	103	
161	JNK2	CMGC	32	31	32	108	120	114	
162	JNK3	CMGC	30	32	31	108	110	109	
163	KIT A829P	TK	107	92	100	123	104	113	
164	KIT D816H	TK	82	79	81	114	110	112	
165	KIT D816V	TK	64	66	65	90	82	86	
166	KIT T670I	TK	99	91	95	96	76	86	
167	KIT V559D	TK	75	76	76	111	113	112	
168	KIT V559D/T670I	TK	102	107	105	124	118	121	
169	KIT V559D/V654A	TK	59	95	77	108	85	96	
170	KIT V560G	TK	35	46	41	95	83	89	
171	KIT V654A	TK	68	95	81	102	105	103	
172	KIT wt	TK	51	52	52	119	107	113	
173	LCK	TK	35	36	35	97	85	91	
174	LIMK1	TKL	97	94	95	102	93	97	
175	LIMK2	TKL	101	93	97	100	89	95	
176	LRRK2 G2019S	TKL	42	39	41	18	14	16	
177	LRRK2 I2020T	TKL	71	65	68	40	41	40	
178	LRRK2 R1441C	TKL	58	61	59	41	35	38	
179	LRRK2 wt	TKL	69	67	68	34	37	36	
180	LTK	TK	74	90	82	10	10	10	
181	LYN	TK	86	85	85	138	137	137	
182	MAP3K10	STE	100	102	101	105	95	100	
183	MAP3K11	STE	89	81	85	88	74	81	
184	MAP3K7/MAP3K7IP1	STE	82	83	83	69	61	65	
185	MAP3K1	STE	105	89	97	87	81	84	
186	MAP3K9	STE	77	72	74	88	82	85	
187	MAP4K2	STE	100	103	101	88	81	85	
188	MAP4K4	STE	107	86	97	99	83	91	
189	MAP4K5	STE	104	90	97	98	89	94	
190	MAPKAPK2	CAMK	90	94	92	98	79	88	
191	MAPKAPK3	CAMK	120	96	108	103	92	98	
192	MAPKAPK5	CAMK	94	88	91	90	88	89	
193	MARK1	CAMK	111	81	96	109	84	97	
194	MARK2	CAMK	77	78	77	79	91	85	
195	MARK3	CAMK	111	92	101	100	83	91	
196	MARK4	CAMK	84	80	82	83	86	84	
197	MATK	TK	202	202	202	117	103	110	
198	MEK1	STE	114	137	125	101	70	86	
199	MEK2	STE	95	86	91	95	80	87	
200	MEKK2	STE	92	91	92	35	33	34	
201	MEKK3	STE	84	83	83	24	23	24	
202	MELK	CAMK	63	65	64	97	85	91	
203	MERTK	TK	116	131	123	94	104	99	
204	MET D1228H	TK	102	98	100	98	93	96	
205	MET D1228N	TK	106	106	106	112	108	110	
206	MET F1200I	TK	99	102	100	108	106	107	
207	MET M1250T	TK	111	95	103	102	90	96	
208	MET wt	TK	99	101	100	95	96	96	
209	MET Y1230A	TK	96	109	103	105	108	107	
210	MET Y1230C	TK	99	93	96	100	102	101	
211	MET Y1230D	TK	97	91	94	98	96	97	
212	MET Y1230H	TK	104	105	104	100	102	101	
213	MET Y1235D	TK	113	110	111	117	113	115	
214	MINK1	STE	105	97	101	100	104	102	
215	MKK6 S207D/T211D	STE	100	120	110	90	99	95	
216	MKNK1	CAMK	107	91	99	99	94	96	

217	MKNK2	CAMK	83	70	76	79	69	74	
218	MST1	STE	100	99	100	104	105	104	
219	MST2	STE	98	93	96	108	98	103	
220	MST3	STE	100	85	92	93	79	86	
221	MST4	STE	99	105	102	111	100	105	
222	mTOR	ATYPICAL	93	90	91	93	89	91	
223	MUSK	TK	14	9	12	72	60	66	
224	MYLK	CAMK	62	56	59	68	56	62	
225	MYLK2	CAMK	110	93	101	114	104	109	
226	MYLK3	CAMK	106	94	100	108	95	102	
227	NEK1	OTHER	53	59	56	88	83	85	
228	NEK11	OTHER	101	89	95	85	88	86	
229	NEK2	OTHER	96	85	90	104	94	99	
230	NEK3	OTHER	90	77	83	74	60	67	
231	NEK4	OTHER	102	93	97	99	93	96	
232	NEK6	OTHER	108	101	105	93	96	94	
233	NEK7	OTHER	128	117	123	114	84	99	
234	NEK9	OTHER	39	31	35	114	100	107	
235	NIK	STE	104	92	98	94	77	86	
236	NLK	CMGC	116	119	117	111	88	99	
237	p38-alpha	CMGC	112	86	99	86	82	84	
238	p38-beta	CMGC	107	98	102	108	97	102	
239	p38-delta	CMGC	106	94	100	99	90	94	
240	p38-gamma	CMGC	103	77	90	88	86	87	
241	PAK1	STE	102	99	100	106	99	102	
242	PAK2	STE	105	92	99	110	99	105	
243	PAK3	STE	103	99	101	97	98	97	
244	PAK4	STE	90	92	91	89	84	86	
245	PAK6	STE	105	87	96	91	82	87	
246	PAK7	STE	99	79	89	98	82	90	
247	PASK	CAMK	94	107	100	97	85	91	
248	PBK	OTHER	107	84	95	108	99	103	
249	PCTAIRE1	CMGC	80	68	74	98	96	97	
250	PDGFR-alpha D842V	TK	54	55	55	97	89	93	
251	PDGFR-alpha T674I	TK	78	78	78	93	94	94	
252	PDGFR-alpha V561D	TK	101	103	102	112	108	110	
253	PDGFR-alpha wt	TK	35	36	35	87	72	79	
254	PDGFR-beta	TK	28	27	28	85	85	85	
255	PDK1	AGC	91	77	84	88	72	80	
256	PHKG1	CAMK	66	63	65	54	56	55	
257	PHKG2	CAMK	84	88	86	79	73	76	
258	PIM1	CAMK	104	93	99	99	95	97	
259	PIM2	CAMK	107	102	104	101	96	99	
260	PIM3	CAMK	105	99	102	103	98	101	
261	PKA	AGC	110	113	111	91	95	93	
262	PKC-alpha	AGC	68	63	66	76	66	71	
263	PKC-beta1	AGC	104	93	99	61	54	57	
264	PKC-beta2	AGC	88	82	85	80	70	75	
265	PKC-delta	AGC	102	114	108	77	84	80	
266	PKC-epsilon	AGC	101	113	107	77	72	74	
267	PKC-eta	AGC	100	98	99	94	102	98	
268	PKC-gamma	AGC	64	52	58	65	71	68	
269	PKC-iota	AGC	94	103	99	105	96	100	
270	PKC-mu	AGC	106	98	102	90	89	90	
271	PKC-nu	AGC	102	86	94	104	79	91	
272	PKC-theta	AGC	100	101	100	88	80	84	
273	PKC-zeta	AGC	102	114	108	99	97	98	
274	PLK1	OTHER	77	80	78	92	88	90	
275	PLK3	OTHER	105	86	95	93	74	83	
276	PRK1	AGC	69	66	68	90	77	83	
277	PRK2	AGC	110	91	101	96	94	95	
278	PRKD2	CAMK	88	82	85	101	90	96	
279	PRKG1	AGC	98	93	96	88	82	85	
280	PRKG2	AGC	51	45	48	50	41	45	
281	PRKX	AGC	96	74	85	73	56	65	
282	PYK2	TK	54	52	53	63	57	60	
283	RAF1 Y340D/Y341D (untagged)	TKL	100	104	102	87	88	88	
284	RET E762Q	TK	37	32	34	46	40	43	
285	RET G691S	TK	37	35	36	47	42	45	
286	RET M918T	TK	36	30	33	48	38	43	
287	RET R749T	TK	40	32	36	52	33	43	
288	RET R813Q	TK	30	25	28	39	27	33	
289	RET S891A	TK	47	33	40	55	52	54	
290	RET V804L	TK	18	13	16	24	20	22	
291	RET V804M	TK	18	18	18	20	15	17	
292	RET wt	TK	34	32	33	43	36	39	
293	RET Y791F	TK	34	32	33	45	42	43	
294	RIPK2	TKL	92	79	86	105	106	105	
295	RIPK5	TKL	88	84	86	106	97	101	
296	ROCK1	AGC	105	102	104	33	25	29	
297	ROCK2	AGC	111	94	102	36	34	35	
298	RON	TK	97	84	91	111	84	98	
299	ROS	TK	40	41	40	70	65	67	
300	RPS6KA1	AGC	101	78	90	92	76	84	
301	RPS6KA2	AGC	78	89	84	95	94	95	
302	RPS6KA3	AGC	81	97	89	104	88	96	
303	RPS6KA4	AGC	96	88	92	94	77	86	
304	RPS6KA5	AGC	123	120	122	87	80	83	
305	RPS6KA6	AGC	68	68	68	93	93	93	
306	S6K	AGC	113	102	107	104	88	96	
307	S6K-beta	AGC	109	82	96	106	100	103	
308	SAK	OTHER	38	25	31	77	81	79	
309	SGK1	AGC	90	95	93	94	90	92	
310	SGK2	AGC	104	94	99	101	89	95	
311	SGK3	AGC	101	100	100	104	89	96	
312	SLK	STE	87	83	85	103	89	96	
313	SNARK	CAMK	57	49	53	66	65	65	
314	SNF1LK2	CAMK	51	41	46	89	86	88	
315	SNK	OTHER	85	89	87	94	92	93	
316	SRC (GST-HIS-tag)	TK	66	59	62	127	109	118	
317	SRMS	TK	102	90	96	105	93	99	
318	SRPK1	CMGC	92	106	99	92	96	94	
319	SRPK2	CMGC	101	110	106	103	105	104	
320	STK17A	CAMK	69	60	64	71	69	70	
321	STK23	CAMK	92	95	94	90	75	83	
322	STK25	STE	97	86	91	101	91	96	
323	STK33	CAMK	50	48	49	99	89	94	
324	STK39	STE	92	87	90	84	82	83	
325	SYK	TK	84	88	86	91	99	95	
326	TAOK2	STE	40	46	43	63	57	60	
327	TAOK3	STE	111	101	106	92	92	92	
328	TBK1	OTHER	81	75	78	85	72	79	
329	TEC	TK	78	72	75	104	95	100	
330	TGFB-R1	TKL	85	87	86	102	111	107	
331	TGFB-R2	TKL	49	41	45	102	80	91	
332	TIE2 R849W	TK	105	91	98	111	105	108	

333	**TIE2 wt**	**TK**		109	113	111	110	92	101
334	**TIE2 Y1108F**	**TK**		101	105	103	113	109	111
335	**TIE2 Y897S**	**TK**		113	108	111	98	93	95
336	**TLK1**	**AGC**		102	107	105	117	100	108
337	**TLK2**	**AGC**		111	99	105	107	84	96
338	**TRK-A**	**TK**		47	45	46	66	55	60
339	**TRK-B**	**TK**		51	46	48	6	6	6
340	**TRK-C**	**TK**		47	47	47	12	11	12
341	**TSF1**	**OTHER**		4	3	4	77	73	75
342	**TSK2**	**CAMK**		101	113	107	117	109	113
343	**TSSK1**	**CAMK**		55	54	55	92	75	84
344	**TTK**	**OTHER**		56	58	57	84	76	80
345	**TXK**	**TK**		37	37	37	74	63	69
346	**TYK2**	**TK**		17	16	17	0	0	0
347	**TYRO3**	**TK**		112	83	97	100	102	101
348	**VEGF-R1**	**TK**		94	99	96	87	96	91
349	**VEGF-R2**	**TK**		52	57	55	85	83	84
350	**VEGF-R3**	**TK**		98	88	93	106	94	100
351	**VRK1**	**CK1**		94	86	90	107	95	101
352	**WEE1**	**OTHER**		61	61	61	106	84	95
353	**WNK1**	**OTHER**		94	101	97	105	106	105
354	**WNK2**	**OTHER**		71	77	74	96	87	91
355	**WNK3**	**OTHER**		99	81	90	99	97	98
356	**YES**	**TK**		50	57	53	100	104	102
357	**ZAK**	**TKL**		86	77	82	99	94	97
358	**ZAP70**	**TK**		122	119	120	127	103	115
Selectivity Score (< 50 % residual activity):						**0.15**			**0.09**

***Classification of protein kinase families (Manning et al. Science 6 December 2002: Vol. 298 no. 5600 pp. 1912-1934):**
AGC: containing PKA, PKG and PKC families
CAMK: Calcium/Calmoduline-dependent protein kinases
CK1: Casein kinase 1 -like
CMGC: containing CDK, MAPK ,GSK3 and CLK families
TK: Tyrosine Kinase
TKL: Tyrosine Kinase-like
STE: Homologs of Yeast Sterile 7, Sterile 11, Sterile 20 Kinases

This selectivity profiling was performed using the kinase panel of ProQinase GmbH, Freiburg, Germany (www.proqinase.com)

Table S1b: Determination of IC50 for selected kinases

SAR302503 (TG101348)

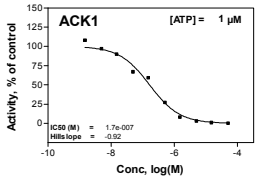

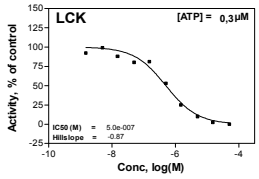

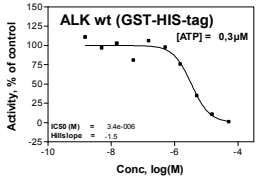

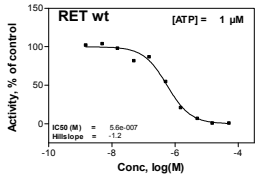

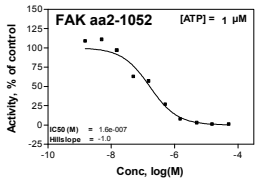

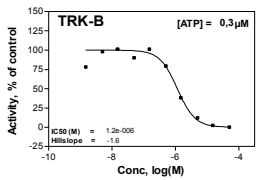

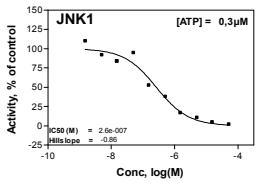

Ruxolitinib

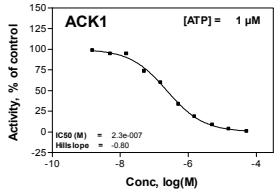

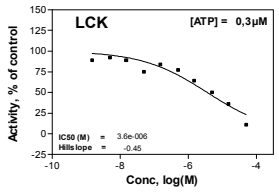

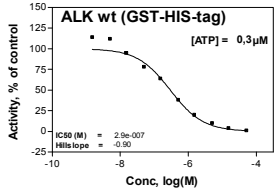

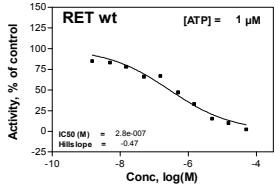

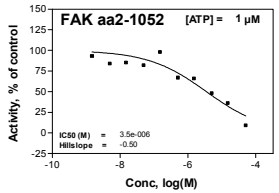

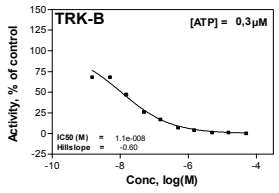

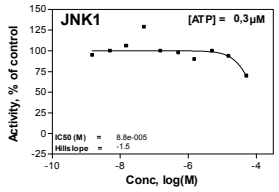

Summary of results

	IC_{50}/nM	
kinase	Ruxolitinib	SAR302503
ACK1	230	170
ALK	290	3400
FAK	3500	160
JNK1	>10000	260
LCK	3600	500
RET	280	560
TRK-B	11	1200
LRRK2 wt	820	1800

LRRK2 inhibition assay